Time-Resolved Diffraction Studies of Ion Exchange: K^+ and Na^+ Exchange into (Al, Ge) Gismondine (GIS) $Na_{24}Al_{24}Ge_{24}O_{96}\cdot 40H_2O$ and $K_8Al_8Ge_8O_{32}\cdot 8H_2O$

Aaron J. Celestian,*,† John B. Parise,†,‡ Carmen Goodell,†
Akhilesh Tripathi,§ and Jonathan Hanson||

Department of Geosciences, Stony Brook University, Stony Brook, New York 11794-2100, Department of Chemistry, Stony Brook University, Stony Brook, New York 11794-3400, Department of Chemistry, Texas A & M University, College Station, Texas 77842-3012, and Department of Chemistry, Brookhaven National Laboratory, Upton, New York 11793-5000

Received August 12, 2003. Revised Manuscript Received March 19, 2004

Time-resolved in situ synchrotron X-ray powder diffraction (XRPD) was used to study ion-exchange mechanisms and pathways in K^+ and Na^+ forms of an aluminogermanate with the zeolite gismondine topology (AlGe−GIS). The Na^+ and K^+ forms differ in their distribution of extraframework cations with the Na^+ ions ordered in the C-centered monoclinic Na−AlGe−GIS of unit-cell dimensions $a = 14.490(3)$ Å, $b = 9.3840(2)$ Å, $c = 23.530(5)$ Å, and $\beta = 105.90(3)°$ and K^+ ions disordered in the I-centered monoclinic K−AlGe−GIS of unit-cell dimensions $a = 10.311(2)$ Å, $b = 9.749(1)$ Å, $c = 10.238(1)$ Å, and $\beta = 90.000(2)°$. Rietveld structure refinements indicate K^+ first occupies sites K2, K4, and K6 in the [101] channel of the Na−AlGe−GIS structure. After 10% (±2%) K^+ exchange into the [$\bar{1}$01] channel, the *I*2/*a* unit cell forms and subsequent replacement of Na^+ is consistent with site independent exchange along the [$\bar{1}$01] and [201] channels. Ion exchange proceeded to approximately 90% (±1%) substitution of K^+ into Na−AlGe−GIS within the course of the experiment. However, in the reverse exchange of Na^+ into the K−AlGe−GIS, an abrupt growth of Na−AlGe−GIS occurred at 4.5% (±3.5%) Na^+ exchange and ended at 10% (±2.5%) Na^+ exchange. Bond valence calculations demonstrate that K^+ has a stronger interaction with framework O^{2-} (0.423 v.u.) than Na^+ (0.242 v.u.) and the valence matching principle shows that Na^+ has a stronger affinity to interstitial H_2O. These results imply that the AlGe−GIS structure has a preference for K^+ as the charge-balancing extraframework cation.

Introduction

Naturally occurring aluminosilicate zeolites are open frameworks composed of corner-connected TO_4 (T = Al, Si) tetrahedra.[1] The negative charge introduced by the substitution of Al^{3+} into a silicate proto-framework is balanced by extraframework cations occupying sites in the rings and channels of the zeolite. Zeolites are a subclass of microporous materials or molecular sieves, a general term given to synthetic frameworks possessing pores and channels on the molecular scale, which imparts the ability to discriminate between molecules and exchangeable cations based upon the relative size of the channels for a particular framework type. Some framework geometries can accommodate a variety of main group elements and the substitution by other group III and IVA elements, such as Ga for Al and Ge for Si. These substitutions, while maintaining the overall framework topology, can lead to different T^{3+}/T^{4+} ratios which may enhance the ion-exchange capacity and alter framework geometry that can affect ion-exchange properties. Because of their potential for selectivity, microporous materials are used in industry and in environmental applications such as in gas separation,[2] in catalytic cracking,[3] and as water softeners.[4] Many environmental uses focus on molecular sieving properties[5] to separate heavy-metal cations from the natural systems. This utility in decontaminating soils and groundwaters[6−11] depends critically on struc-

* To whom correspondence should be addressed. E-mail: aaron.celestian@stonybrook.edu.
† Department of Geosciences, Stony Brook University.
‡ Department of Chemistry, Stony Brook University.
§ Department of Chemistry, Texas A & M University.
|| Department of Chemistry, Brookhaven National Lab.

(1) Bish, D. L.; Ming, D. W. *Reviews in Mineralogy and Geochemistry*; The Mineralogical Society of America: Washington, 2001; Vol. 45.
(2) Kuznicki, S. M.; Bell, V. A.; Nair, S.; Hillhouse, H. W.; Jacubinas, R. M.; Braunbarth, C. M.; Toby, B. H.; Tsapatsis, M. *Nature* **2001**, *412*, 720−724.
(3) Corma, A. *Chem. Rev.* **1997**, *97*, 2373−2419.
(4) Carr, S. W.; Gore, B.; Anderson, M. W. *Chem. Mater.* **1997**, *9*, 1927−1932.
(5) Breck, D. W. *Zeolite Molecular Sieves, Structure, Chemistry and Uses*; Wiley-Interscience: New York, 1974.
(6) Dyer, A.; Abou-Jamous, J. K. *J. Radioanal. Nucl. Chem.* **1997**, *224*, 59−66.
(7) Olguin, M. T.; Solache-Rios, M.; Acosta, D.; Bosch, P.; Bulbulian, S. *Microporous Mesoporous Mater.* **1999**, *28*, 377−385.
(8) Misaelides, P.; Godelitsas, A.; Filippidis, A.; Charistos, D.; Anousis, I. *Sci. Total Environ.* **1995**, *173*, 237−246.
(9) Vidya, K.; Dapurkar, S. E.; Selvam, P.; Badamali, S. K.; Gupta, N. M. *Microporous Mesoporous Mater.* **2001**, *50*, 173−179.
(10) Rodriguez-Iznaga, I.; Gomez, A.; Rodriguez-Fuentes, G.; Benitez-Aguilar, A.; Serrano-Ballan, J. *Microporous Mesoporous Mater.* **2002**, *53*, 71−80.
(11) Zamzow, M. J.; Eichbaum, B. R.; Sandgren, K. R.; Shanks, D. E. *Sep. Sci. Technol.* **1990**, *25*, 1555−1569.

10.1021/cm034746i CCC: $27.50
Published on Web 04/29/2004

tural properties of the molecular sieve, including how their structural properties change during the ion-exchange process. A basic understanding of the structural effects of ion exchange is therefore a necessary complement to bulk analysis of ion-exchange capacity.[5,12,13]

Most structural research on ion exchange in microporous materials is conducted in a static context. Crystals are mixed with an electrolyte in a closed environment, removed after some time, and studied for chemical composition and/or structural changes. These ex situ structural studies of ion-exchanged crystals show the average cation sites, which may have changed upon removal from the ion-exchange solution. They do provide precise structural determinations, however, and if we presume they accurately reflect the state of the solid in the ion-exchange solution, ex situ studies can help in deriving pathways for ion exchange.[14,15] Ex situ ion-exchange structure solution or refinement from single-crystal or powder XRD data of disordered structures is difficult. Those techniques are hindered by the fact that they cannot observe the kinetics of ion exchange on a short enough time scale to follow the dynamics of mobile cations. They also do not offer direct evidence to allow construction of models explaining the step-by-step mechanism of ion exchange. For example, in materials containing multiple sites for ion exchange, the loading/unloading of these sites can affect the framework structure.[16,17] The pathways these guest species take to exchange the host species can affect the overall loading capacity and ionic selectively of microporous materials. Following this process on short time scales allows us to track structural changes and their effect on ion exchange directly without removing the solid from the exchange solution. Combined with ex situ studies, which allow precise determinations of crystal structure and provide realistic restraints on interatomic distances to supplement less precise time-resolved work, complementary in situ work provides a more complete picture of the ion-exchange process.

Thermodynamic calculations describe the selective nature of ion-exchange reactions at equilibrium,[18] but cannot show mobility pathways as these equations are path-independent. The benefit of studying these reactions in situ include the ability to observe how the structure changes due to the introduction of new guest species, how guest species migrate, and to resolve if guest species are site-selective exchangers. In situ ion exchange permits resolution of cation loading dynamics by quantifying the amount of exchanging guest species necessary to induce structural changes and how exchange rates are affected by increased cation loading. Recently, hypotheses addressing how cation loading dynamics affect the progress of ion exchange were posited by Lee et al.[14,16] Those authors described a possibility for site-specific substitution in zeolites, but could not resolve the directions in which cations were migrating into the structure.

Background to the AlGe−GIS Structures. Since the structure determination of gismondine by Fisher,[19,20] ion-exchange studies of natural (Al, Si) and synthetic (Al, Ge) framework variants have shown that this material has potential applications for use as detergent builders.[18] The bulk of these studies have been carried out at equilibrium, and thus the thermodynamics have been well-characterized under various ion-exchange conditions.[18,21] Ex situ X-ray diffraction studies illustrate structural transformations after the exchange process and serve a vital role in understanding structural and atomic relations of framework and extraframework species. Such structural investigations[22−24] show the flexibility of the gismondine framework in a diverse range of cation-exchange studies.

Tripathi et al.[23] first synthesized Na^+ and K^+ forms of AlGe−GIS ($K_8Al_8Ge_8O_{32}\cdot 8H_2O$ and $Na_{24}Al_{24}Ge_{24}O_{96}\cdot 40H_2O$, respectively) with ordered Al and Ge occupying the available T-sites and with K^+ and Na^+ as charge-balancing cations occupying extraframework sites. The abbreviation GIS refers to the International Zeolite Association structure code[25] for gismondine. Although GIS can crystallize in monoclinic, orthorhombic, or tetragonal crystal systems, the idealized unit-cell is tetragonal, I_1/amd with $a = 9.8$ Å and $c = 10.2$ Å.[25] The topology of GIS consists of two perpendicular intersecting eight-membered ring (8MR) channels (Figure 1). The framework is interconnected by a 4MR of ordered Al and Ge tetrahedra in a ratio of 1:1. Contained in the (010) plane of both forms of GIS are two sets of double crankshaft chains that are oriented at right angles with respect to each other.

In Na−AlGe−GIS,[23] with unit-cell dimensions $a =$ 14.490(3) Å, $b = 9.940(2)$ Å, $c = 23.530(5)$ Å, $\beta = 105.90(3)°$, and space group $C2/c$, Na^+ is near the walls of the 8MR along the $[\bar{1}01]$ direction in 6-fold coordination, bonding to two framework O^{2-} and to four H_2O molecules on average. The H_2O sites are fully occupied near the center of the $[\bar{1}01]$ channel and 50% occupied along the center of the [201] channel. The bond distance of Na^+ to O^{2-}/H_2O ranges from 2.3 to 3.0 Å. The double crankshaft chains of Na−AlGe−GIS are twisted, opening pockets in the channels for Na^+ to bond with framework O^{2-} (Figure 2) and allowing Na^+ to be fully ordered. Theoretically placing K^+ into the Na^+ sites results in unacceptable bond distances due to the larger radius of K^+. Rather the larger K^+ occupies the center of the 8MR channels to create a stable bonding environment.

In K−AlGe−GIS,[23] with unit-cell dimensions $a =$ 10.311(2) Å, $b = 9.749(1)$ Å, $c = 10.225(6)$ Å, $\beta = 90.000-$

(12) Helfferich, F. *Ion Exchange*; McGraw-Hill Book Company, Inc.: New York, 1962.
(13) Sherry, H. S. *J. Phys. Chem.* **1966**, *70*, 1158−1168.
(14) Lee, Y. J.; Carr, S. W.; Parise, J. B. *Chem. Mater.* **1998**, *10*, 2561−2570.
(15) Parise, J. B.; Prince, E. *Mater. Res. Bull.* **1983**, *18*, 841−852.
(16) Lee, Y. J.; Kim, S. J.; Schoonen, M. A. A.; Parise, J. B. *Chem. Mater.* **2000**, *12*, 1597−1603.
(17) Lee, Y.; Cahill, C. L.; Hanson, J. C.; Parise, J. B.; Carr, S. W.; Myrick, M. L.; Preckwinkel, U. V.; Phillips, J. C. In *12th International Zeolite Conference*, Vol. 4; Materials Research Society: Warrendale, PA, 1998.
(18) Allen, S.; Carr, S.; Chapple, A.; Dyer, A.; Heywood, B. *Phys. Chem. Chem. Phys.* **2002**, *4*, 2409−2415.
(19) Fischer, K. *Am. Mineral.* **1963**, *48*, 664−672.
(20) Fischer, K. F.; Schramm, V. *Adv. Chem. Ser.* **1971**, 250−258.
(21) Adams, C. J.; Araya, A.; Cunningham, K. J.; Franklin, K. R.; White, I. F. *J. Chem. Soc., Faraday Trans.* **1997**, *93*, 499−503.
(22) Bauer, T.; Baur, W. H. *Eur. J. Mineral.* **1998**, *10*, 133−147.
(23) Tripathi, A.; Parise, J. B.; Kim, S. J.; Lee, Y.; Johnson, G. M.; Uh, Y. S. *Chem. Mater.* **2000**, *12*, 3760−3769.
(24) Nery, J. G.; Mascarenhas, Y. P.; Cheetham, A. K. *Microporous Mesoporous Mater.* **2003**, *57*, 229−248.
(25) Baerlocher, C.; Meier, W. M.; Olson, D. H. *Atlas of Zeolite Framework Types*; Fifth Revised ed.; Elsevier: New York, 2001.

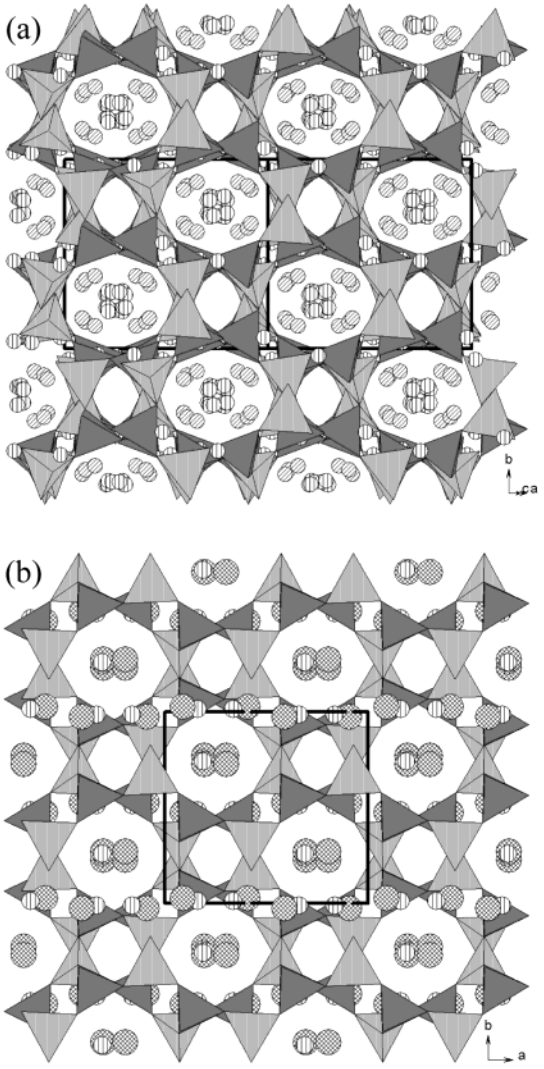

Figure 1. Polyhedral representation of the (a) ordered Na−AlGe−GIS (view down [$\bar{1}$01]) and the (b) disordered K−AlGe−GIS (view down [001]) frameworks. Unit cell is outlined in black, Ge−O tetrahedra are dark gray, Al−O tetrahedra are light gray, vertically hatched spheres are H_2O (O), diagonal hatching spheres are Na^+, and cross-hatched spheres are K^+.

(2) Å, and space group *I*2/*a*, K^+ is disordered with H_2O over two distinct crystallographic sites, each having an occupancy of 50%. These species are near the center of the 8MR along [100] and [001] bonding to five framework O^{2-} and to three channel H_2O molecules. The larger K^+ radius allows K^+-O^{2-} bonds across the diameter of the channels with O^{2-}/H_2O distances between 2.74 and 3.37 Å.

The unit-cell and atomic position relationships between K−AlGe−GIS and Na−AlGe−GIS is described by a 4 × 4 transformation matrix and by four unique translation vectors (methods for obtaining these are described elsewhere[26,27]). To transform K−AlGe−GIS (*I*2/*a*) into the Na−AlGe−GIS (*C*2/*c*) basis, matrix **P** = [(−1 0 −1 −0.5)(0 1 0 0)(−1 0 2 −0.5)(0 0 0 1)] was derived by geometric methods. By multiplying the inverse of this matrix (**P**$^{-1}$ = **Q**) to all lattice positions, three

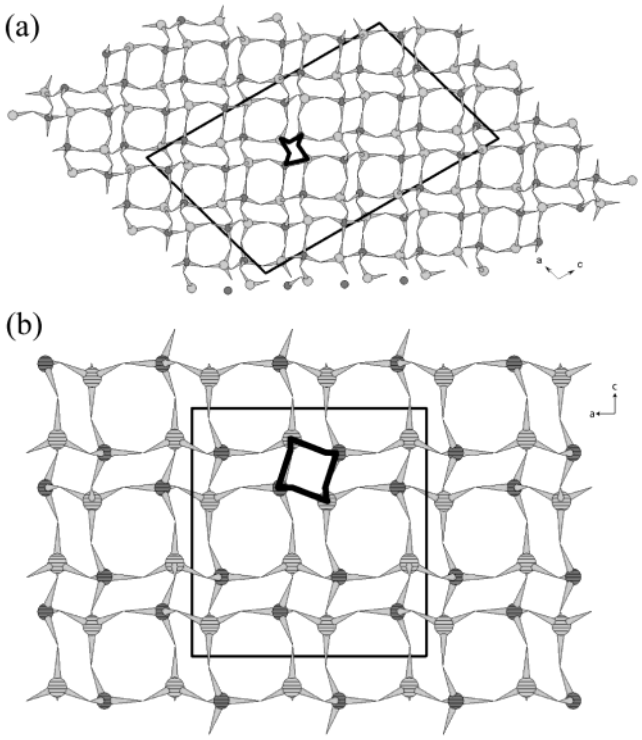

Figure 2. Ball-and-stick representation along the *b*-axis of the (a) ordered Na−AlGe−GIS and (b) disordered K−AlGe−GIS frameworks. Bold box outline in the *C*2/*c* unit cell shows the distortion of the 4MR at the intersection of the perpendicular double crankshaft chains relative to the *I*2/*a* unit cell. Unit-cell outline in thin solid black, Ge atoms are dark gray, Al atoms are light gray, and Na^+, K^+, O^{2-}, and H_2O (O) are omitted for clarity.

unique vectors serving as atomic position translation vectors [$\mathbf{c}_1$ = (−0.1667 0 −0.3333 1), $\mathbf{c}_2$ = (−0.8333 0 −0.6667 1), $\mathbf{c}_3$ = (−0.5 0 0 1) obtained from the eight-corner lattice points] and one lattice centering translation vector [**I** = (−0.6667 0.5 −0.3333 1) obtained from the body-center lattice point] were calculated. To transform K−AlGe−GIS atomic positions to the Na−AlGe−GIS (*C*2/*c*) basis, each atomic fractional position must be multiplied by **Q** and the resultant **Z** is added [**Z** + (**c**$_1$ + **I**), **Z** + (**c**$_2$ + **I**), and **Z** + (**c**$_3$ + **I**)] to generate three new atomic positions in the Na−AlGe−GIS (*C*2/*c*) basis per atom from the *I*2/*a* basis. These calculations illustrate the mathematical relationship between K−AlGe−GIS, which has approximately 3 times less unit-cell volume, and Na−AlGe−GIS, which has eight more H_2O molecules per unit-cell volume in the *C*2/*c* basis. Atomic positions of the transformed K−AlGe−GIS structure into the *C*2/*c* basis are shown in Table 1, which contains all known possible locations of extraframework species.

The present study examines the ion exchange of K^+ and Na^+ into the Na and K forms of the aluminogermanate microporous material. The selection of the GIS topology was motivated by its well-characterized structure, complex order−disorder relationships of extraframework cations, and the possible applications of the aluminogermanate form as a detergent builder. Experiments using time-resolved in situ XRPD were preformed to demonstrate how cations migrate through the crystal structure and how the structure transforms from the super-group to sub-group. Although this technique

(26) *International Tables for Crystallography*; D. Reidel Publishing Company: Boston, 1987; Vol. A.
(27) O'Keeffe, M.; Hyde, B. G. *Crystal Structures*; Mineralogical Society of America: Washington, 1996; Vol. 1.

Table 1. Atomic Coordinates for the Transformed *I*2/*a* into the *C*2/*c* Unit-Cell Basis Including Na^+ Positions

atom	site	p[a]	*x*	*y*	*z*	*U*(eq)[b]
A11	8f	1	−0.5080	0.3397	−0.5665	0.0200
A12	8f	1	−1.1746	0.3397	−0.8999	0.0200
A13	8f	1	−0.8413	0.3397	−0.2332	0.0200
Ge1	8f	1	−0.6899	0.4136	−0.6846	0.0200
Ge2	8f	1	−1.3565	0.4136	−1.0180	0.0200
Ge3	8f	1	−1.0232	0.4136	−0.3513	0.0200
K1	8f	q	−0.59	0.4726	−0.8231	0.0500
K2	8f	q	−0.5887	0.7723	−0.7167	0.0500
K3	8f	q	−1.2567	0.4726	−1.1564	0.0500
K4	8f	q	−1.2554	0.7723	−1.0500	0.0500
K5	8f	q	−0.9233	0.4726	−0.4898	0.0500
K6	8f	q	−0.9220	0.7723	−0.3834	0.0500
Na1	8f	q	−0.0292	1.3393	0.4444	0.0500
Na2	8f	q	0.2176	0.8613	0.3840	0.0200
Na3	8f	q	0.0190	1.1183	3.2960	0.0200
O1	8f	1	−0.57733	0.4337	−0.6296	0.0200
O10	8f	1	−1.0624	0.5793	-0.3732	0.0200
O11	8f	1	−1.0122	0.3294	-0.4154	0.0200
O12	8f	1	−1.1047	0.3213	-0.3248	0.0200
O2	8f	1	−0.7291	0.5793	-0.7065	0.0200
O3	8f	1	−0.6789	0.3294	-0.7487	0.0200
O4	8f	1	−0.7714	0.3213	-0.6581	0.0200
O5	8f	1	−1.2440	0.4337	-0.9629	0.0200
O6	8f	1	−1.3958	0.5793	-1.0398	0.0200
O7	8f	1	−1.3456	0.3294	-1.0820	0.0200
O8	8f	1	−1.4380	0.3213	-0.9915	0.0200
O9	8f	1	−0.9107	0.4337	-0.2962	0.0200
O40[c]	8f	q	−0.548533	0.4837	-0.7982	0.0500
O41[c]	8f	q	−0.5686	0.7589	-0.7413	0.0500
O42[c]	8f	q	−1.2152	0.4837	-1.1315	0.0500
O43[c]	8f	q	−1.2352	0.7589	-1.0747	0.0500
O44[c]	8f	q	−0.8819	0.4837	-0.4648	0.0500
O45[c]	8f	q	−0.9019	0.7589	-0.4080	0.0500

[a] p = site occupancy. q = unrefined occupancies but serves as a starting position for atomic sites. [b] Isotropic atomic displacement parameters ($Å^2 \times 10^2$). [c] Interstitial water molecules (H^+ positions not calculated).

requires very high resolution diffraction data and employs a large number of constraints and restraints during structure refinement, it provides unique information of cation mobility during ion exchange that cannot be obtained conveniently with other diffraction techniques.

Experimental Section

Single crystals of Na−AlGe−GIS and K−AlGe−GIS were synthesized according to methods described by Tripathi et al.[23] The Na−AlGe−GIS preparation yielded octahedral GIS and cubic (Al, Ge) sodalite (SOD) crystals. On average, each Na−AlGe−GIS crystal was 80 μm on edge. Na−AlGe−SOD crystals had an approximate 5−μm edge length. XRPD on a Scintag PAD-X automated diffractometer was used for phase characterization. No mechanical phase separation was performed in isolating either Na−AlGe−GIS or Na−AlGe−SOD. Rietveld refinement[28] using the Scintag XRPD data showed that 99% of the sample consisted of Na−AlGe−GIS. Diffraction studies were carried out on multiple samples to eliminate any phase selection bias. K−AlGe−GIS preparation yielded single octahedral crystals with an approximate edge length of 80 μm. Powder diffraction phase analysis did not show any impurity phase present, which is consistent with the results of Tripathi et al.[23]

Crystals of Na−AlGe−GIS and K−AlGe−GIS were ground separately in an agate mortar and pestle to a fine powder. Approximately 5 mg of the powders was loaded individually into 0.5- and 0.7-mm quartz capillaries. A matrix of glass wool was placed on either side of the powder to contain the sample.

The Small Environment Cell for Real Time Studies (SECReTS)[29] allows a solution to pass through a powder sample mounted on a diffractometer. The construction is a modified goniometer mount that fixes a capillary into a plumbing system.[30] Before the ion-exchange solution is passed through the capillary, deionized water is injected. Then, a solution containing the exchanging electrolyte is pushed by an overpressure (adjusted to be between 10 and 15 psi) of N_2 gas through the capillary. Slowly introducing the exchanging cation facilitates observation of the initial ion-exchange dynamics.

Ion-exchange solutions were prepared at room temperature and ambient pressure. KCl and 200 mL of deionized H_2O were mixed to make 0.01 M KCl solution. NaCl and 200 mL of deionized H_2O were mixed to make 0.5 M NaCl solution.

In situ ion exchange was conducted at the X7B beamline of the National Synchrotron Light Source (NSLS) at Brookhaven National Laboratory. This beamline offers greater flux, brightness, and collimation of X-rays as compared to conventional sealed tube sources.[31] These factors are particularly important when studying the appearance and disappearance of weak reflections resulting from subtle changes in the structure during ion exchange. The X7B goniometer is equipped with a rotating ϕ circle set at a fixed $\chi = 90°$. The sample was rotated ($\Delta\phi = 60°$) during data collection to help improve powder averaging and then moved back to the starting position before the next frame is acquired. Diffracted X-ray data were collected on a MAR 345 imaging plate (IP) detector with a built-in scanner for online reading. Erasing, exposing, and reading the IP limits the time resolution to about 2.5 min.

Data were acquired for 60-s exposures with 1°/s ϕ oscillation for each frame. The K^+ for Na−AlGe−GIS exchange proceeded for 9.25 h. The Na^+ for K−AlGe−GIS exchange proceeded for 4 h.

After data collection, IP data were calibrated and integrated using the program Fit2D.[32−35] Integrated data were converted to DiffracPlus and CPI format by the program ConvX.[36] These formats were used in the programs EVA (data evaluation and plotting software),[37] CRYSFIRE (automated unit-cell determination software),[38] XFIT (peak-fitting software),[39] and TOPAS (Rietveld refinement software)[40] for the processing of data for structure refinement. Structure models for each phase were refined using the Rietveld method[28] in TOPAS to obtain unit-cell parameters and, when possible, occupancies of extraframework cations.

Results

The time-resolved data of K^+ for Na−AlGe−GIS and Na^+ for K−AlGe−GIS (Figures 3 and 4) document the presence of new peaks and peak splittings in diffraction patterns as ion exchange proceeded. Rietveld refinement used the models for the pure end-member AlGe materi-

(28) Rietveld, H. M. *J. Appl. Crystallogr.* **1969**, *2*, 65−71.
(29) Norby, P.; Cahill, C.; Koleda, C.; Parise, J. B. *J. Appl. Crystallogr.* **1998**, *31*, 481−483.
(30) Norby, P. In *Mater. Sci. Forum* **1996**, *228−231*, 147−152.
(31) Department of Chemistry, N.S.L.S., Brookhaven National Laboratory: http://www.chemistry.bnl.gov/SciandTech/CRS/X7b/x7bdes.html.
(32) Hammersley, A. P. *FIT2D: V9.129 Reference Manual V3.1*; ESRF: Grenoble, France, 1998.
(33) Hammersley, A. P.; Svensson, S. O.; Thompson, A. *Nucl. Instrum. Methods* **1994**, *A346*, 312−321.
(34) Hammersley, A. P.; Svensson, S. O.; Thompson, A.; Graafsma, H.; Kvick, A.; Moy, J. P. *Rev. Sci. Instrum.* **1995**, *66*, 2729−2733.
(35) Hammersley, A. P.; Svensson, S. O.; Hanfland, M.; Finch, A. N.; Hausermann, D. *High-Pressure Res.* **1996**, *14*, 235−248.
(36) Bowden, M., ConvX program, 1998. http://ccp14.minerals.csiro.au/ccp/web-mirrors/convx/.
(37) EVA: data evaluation and plotting software, 4.0.0.2 ed. Bruker AXS: Karlsruhe, Germany, 1998.
(38) Shirley, R. CRYSFIRE program, 9.33 ed. University of Surrey: Guildford, U.K., 2002.
(39) Cheary, R. W.; Coel, A. A. XFIT and FOURYA Daresbury Laboratory: Warrington, England, 1996.
(40) TOPAS software. Bruker AXS: Karlsruhe, Germany, 2000.

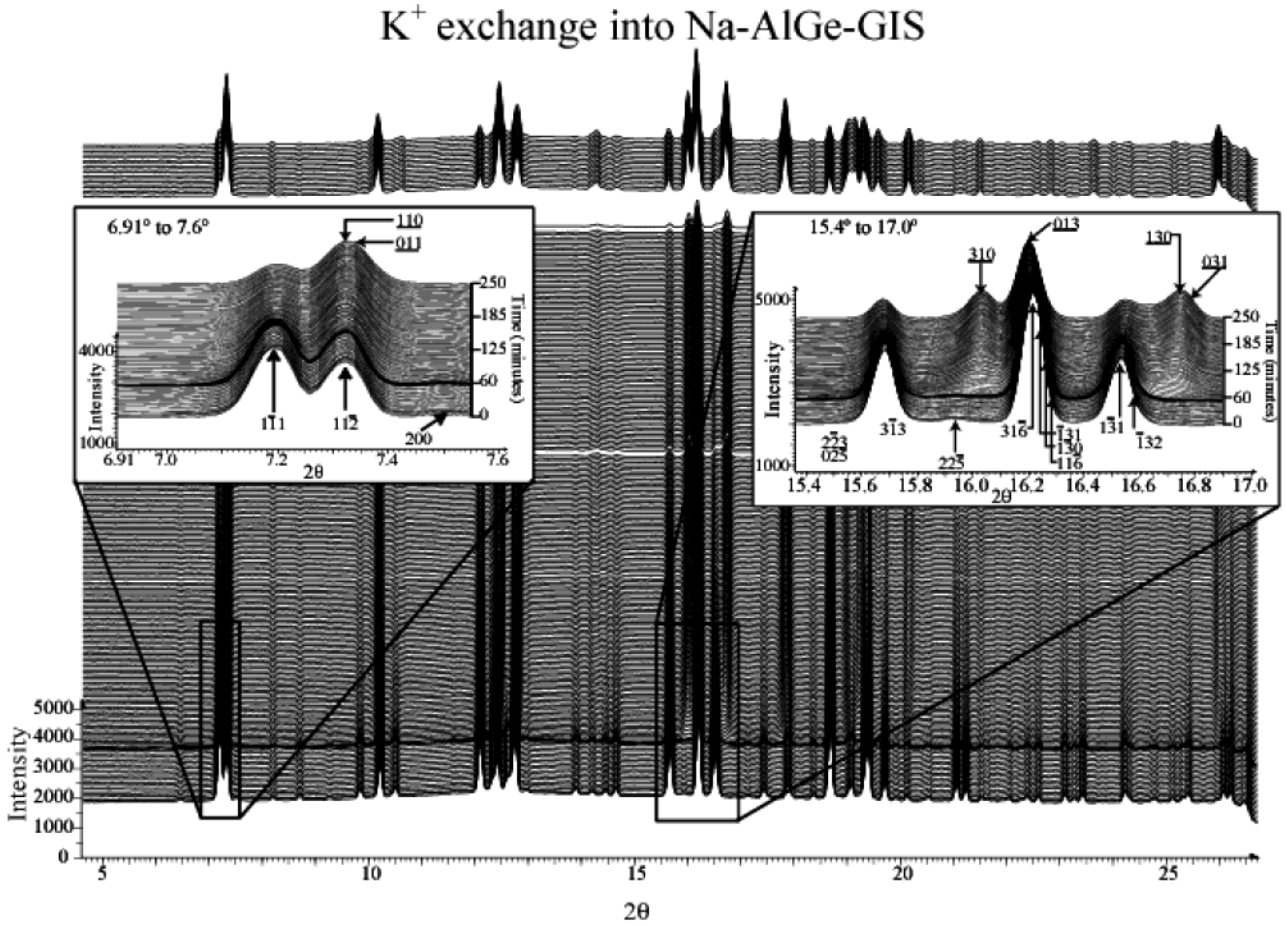

Figure 3. Time-resolved in situ X-ray diffraction patterns for the K^+ ion exchange into Na−AlGe−GIS. Bold line profile indicates the onset of ion exchange.

als described in the literature.[23] As exchange proceeded, unit-cell parameters were determined by Rietveld refinement using these models and then Distance Least Squares (DLS) refinement[41] provided atomic positions for the framework atoms and these were fixed during the subsequent refinements. Unit-cell parameters, refined for both phases, showed no variation from the initial parameters (Figures 5 and 6) and were held constant throughout subsequent refinements. Initial Le Bail refinements[42] were used to establish reasonable parameters of peak shape, modeled using a Gaussian and Lorentzian fundamental parameters profile, and for background. Peak shape and background were held constant during subsequent refinements. As a test of the reasonableness of the DLS-derived framework parameters, trial refinements of the framework Al and Ge positional parameters were carried and they showed no significant deviation from the initial parameters; thus, they were held constant throughout subsequent refinements. Fourier difference maps calculated with the DLS-derived models revealed no indication of additional unaccounted electron density (Figure 7).

Extraframework H_2O (modeled using the scattering factor for O^{2-}) in addition to those found in single-crystal studies of Tripathi et al.[23] were located and their positions fixed in subsequent refinements. Atomic isotropic displacement parameters for all atoms were fixed using single-crystal data obtained from Tripathi et al.[23] With these constraints applied, the number of parameters for Rietveld refinement reduced to only occupancy and positional parameters for the extraframework species Na^+, K^+, and H_2O in the K^+ for Na−AlGe−GIS ion-exchange powder profiles. Once positional parameters of extraframework species where determined, they were fixed in future refinements when the diffraction profile contained two phases.

Ion Exchange of K^+ for Na−AlGe−GIS. The onset of ion exchange of K^+ in Na−AlGe−GIS was seen as subtle shifts in peak intensity between the $(1\bar{1}1)$ and $(11\bar{2})$ reflections of Na−AlGe−GIS (Figure 3). Rietveld refinement of the extraframework cation occupancies suggested that, at this point, K^+ substituted for Na^+ preferentially along the $[\bar{1}01]$ channel (atomic sites labeled K2, K4, and K6 from Table 1). This selective substitution continued until 10% (±2%) K^+ exchange, based on Rietveld refinement (Figures 8 and 9) upon which K−AlGe−GIS began to form as evidenced by peak splittings and new peak growth. Once K−AlGe−GIS formed, extraframework atomic positions could not be refined but were fixed in accordance with previously determined structures of K−AlGe−GIS and Na−AlGe−GIS,[23] and refinement of the occupancies only were carried out. The calculated profile matched the measured profile (examples of Rietveld refinement profiles

(41) Baerlocher, C.; Hepp, A.; Meier, W. M. DLS-76 program Institut fur Krstallographie und Petrologie at ETH: Zurich, Switzerland, 1977. http://www.chemistry.bnl.gov/SciandTech/CRS/X7b/x7bdes.html, 2002.

(42) Le Bail, A.; Duroy, H.; Fourquet, J. L. *Mater. Res. Bull.* **1998**, *23*, 447−452.

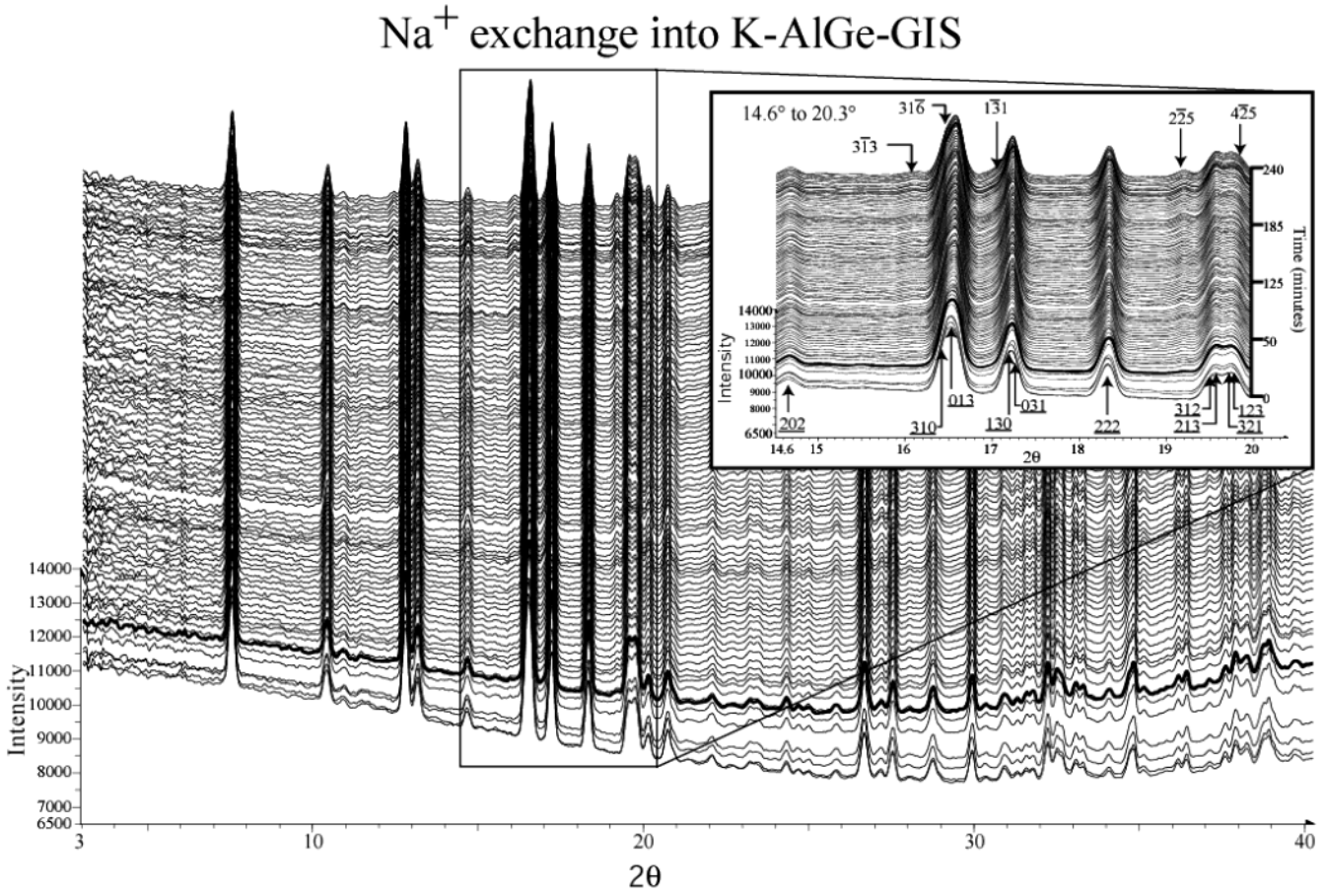

Figure 4. Time-resolved in situ X-ray diffraction patterns for the Na^+ ion exchange into K−AlGe−GIS. Bold line profile indicates the onset of the phase transition.

are shown in Figure 9) and was consistent with a nonspecific site substitution into the Na−AlGe−GIS structure. Refinements converged with a best R_{wp} = 3.41%, R_{bragg} = 3.60%, and GOF = 1.60% at the beginning of the experiment and the worst R_{wp} = 4.3%, R_{bragg} = 4.77%, and GOF = 1.80% was obtained at the end of the experiment. The final refined occupancy of K^+ determines 90% (±1%) exchange (Figure 8).

Ion Exchange of Na^+ for K−AlGe−GIS. In the case of the Na^+ for K−AlGe−GIS exchange, simultaneous refinements of positional and occupancy parameters resulted in unstable and inconsistent values. The lower peak width resolution in the diffraction profiles did not allow independent refinement of the extraframework atomic positions and occupancies. The atomic positions were therefore obtained from published single-crystal data[23] and only occupancy factors were refined when only the K−AlGe−GIS phase was present. Since H_2O, Na^+, and partially occupied K^+-sites have similar X-ray scattering powers, distinctions between sites occupied by these species were made based upon cation-(or water)-to-framework distances and the accurate structures determined from ex situ data collected for hydrated native and ion-exchanged single crystals.[23] Refinements converged at the beginning of the ion exchange with R_{wp} = 0.95%, R_{bragg} = 0.85%, and GOF = 0.68% and at the end of ion exchange with R_{wp} = 1.35%, R_{bragg} = 0.923%, and GOF = 0.91%.

The onset of Na^+ in K−AlGe−GIS ion exchange was after 4.5% (±3.5%) Na^+ substitution based on Rietveld refinements, as a slow growth of the Na−AlGe−GIS reflections. Rietveld refinement of occupancy parameters of all known K^+ and Na^+ sites obtained from single-crystal data[23] was performed to determine the extent of ion exchange (Figure 8). Ion exchange of Na^+ into the K−AlGe−GIS structure only achieved 10% (±2.5%) K^+ replacement based on the refined site occupancies of extraframework positions.

Discussion

The information gained from in situ time-resolved measurements allows us to directly follow the ion-exchange process. The benefit of calculating the percentage of cations present in the channels from structural refinements is unique to this study and increases the reliability and confidence of the derived structural models.

Ion exchange of K^+ into Na−AlGe−GIS proceeded to 90% (±1%) completion based on Rietveld refinement within the time frame of the experiment. Site-specific substitution in sites K2, K4, and K6 (Table 1) into the [$\bar{1}$01] channel direction of Na−AlGe−GIS was observed prior to the formation of K−AlGe−GIS. Na^+ cations were ordered along the [$\bar{1}$01] channel, and once exchanged out of the structure, a local charge deficiency results that must be recouped by K^+ to maintain electroneutrality and long-term structural stability. Site-specific ion exchange continued while the Na−AlGe−GIS unit cell persisted and the ordering of Na^+

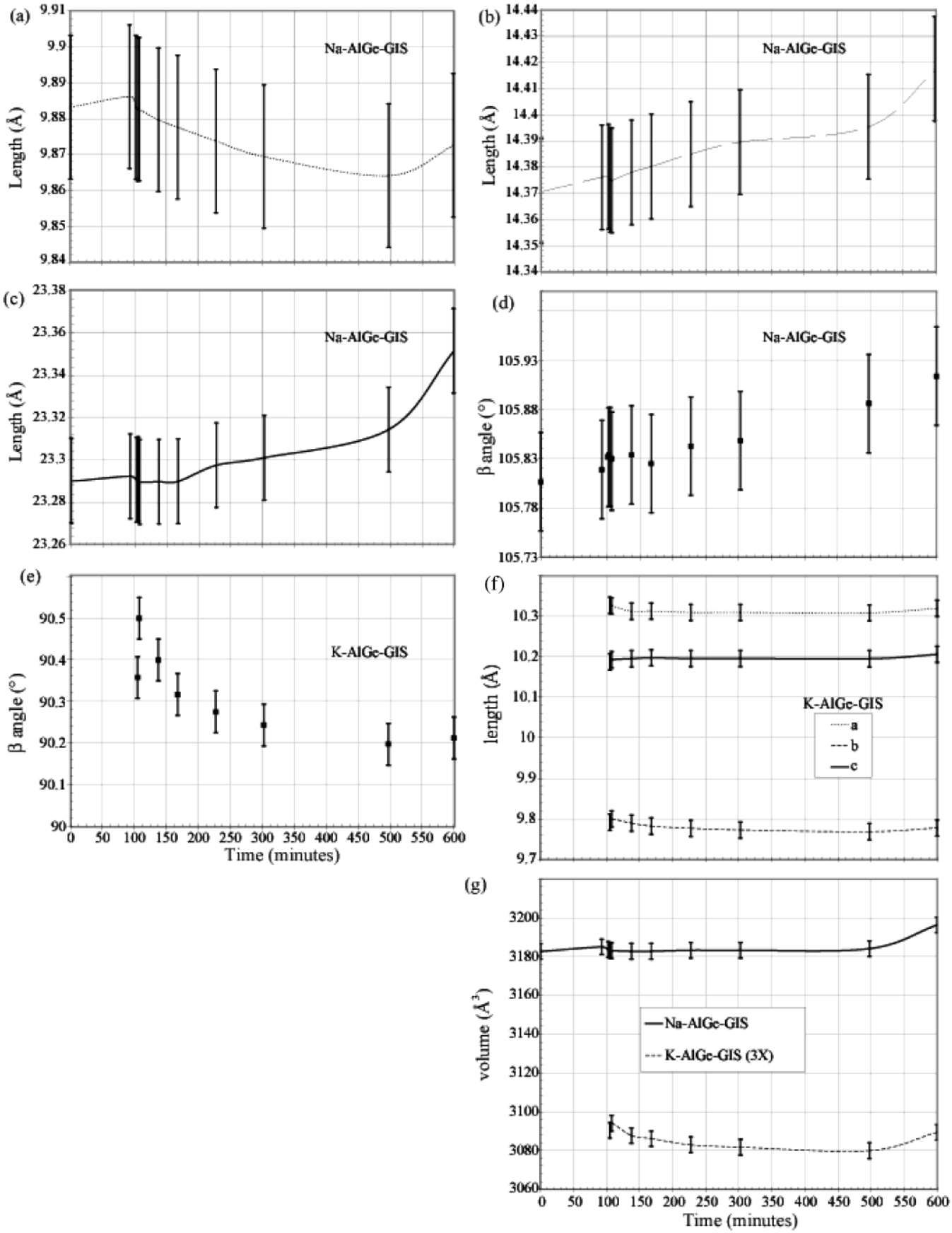

Figure 5. Refined unit-cell parameters and volume changes in Na−AlGe−GIS and K−AlGe−GIS as a function of K^+ ion exchange into Na−AlGe−GIS. (a) Unit-cell length *a* of Na−AlGe−GIS, (b) unit-cell length *b* of Na−AlGe−GIS, (c) unit-cell length *c* of Na−AlGe−GIS, (d) β angle of Na−AlGe−GIS, (e) β angle of K−AlGe−GIS, (f) unit-cell parameters *a*, *b*, and *c* of K−AlGe−GIS, and (g) volumes of both Na and K−AlGe−GIS.

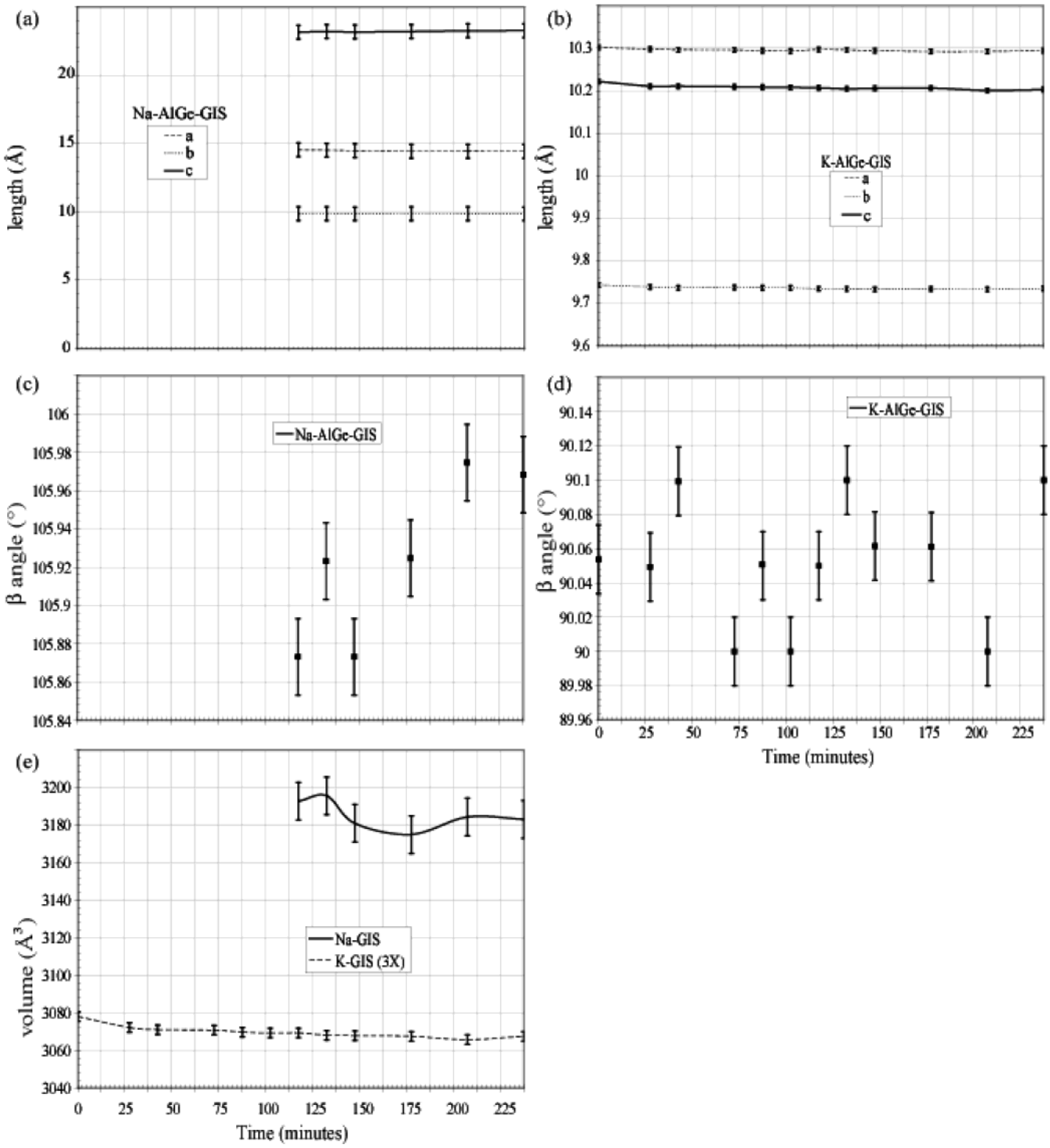

Figure 6. Refined unit-cell parameters and volume changes in K−AlGe−GIS and Na−AlGe−GIS as a function of Na^+ ion exchange into K−AlGe−GIS.

is maintained. Once K−AlGe−GIS forms, Na^+ ordering is no longer preserved and all extraframework positions are disordered. The onset of the K−AlGe−GIS structure increased the number of refinable framework and extraframework positional parameters in the Rietveld refinement, and it was not determined whether site-specific ion exchange continued. Rietveld refinements which included all the parameters resulted in convergence to false minima in the final least-squares cycles. Tripathi et al.[23] modeled an interpreted 50% KNa−AlGe−GIS structure that adopted the *I*2/*a* unit cell and showed K^+, Na^+, and water disordered in both the [100] and [001] channels. Using this model as a guide for further refinement, it was determined that the onset of K−AlGe−GIS stopped site-specific ion exchange, and K^+ substitution into Na−AlGe-GIS was consistent with a random substitution model. At no point was K^+ ordered along the channels in either the K−AlGe−GIS or the Na−AlGe−GIS unit cell. The K^+ for Na−AlGe−GIS ion exchange may have gone to completion, but the allotted

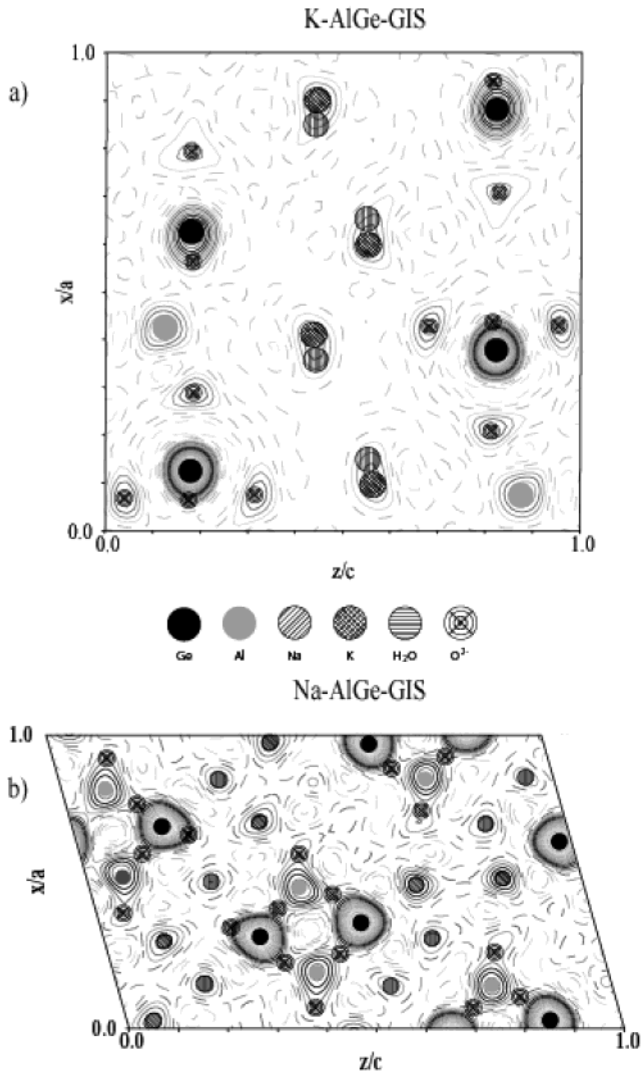

Figure 7. Fourier difference maps for the starting mateials (a) K−AlGe−GIS and (b) Na−AlGe−GIS. Maps are projected perpendicular to the [010] axis and are a superposition of electron density between $0.3 \leq y/b \leq 0.6$. Dashed contour lines represent negative differences between calculated and observed Fourier maps. Symbols represent atomic positions.

beamtime prevented continuation of the experiment. The calculated rate of decelerating ion exchange, assuming constant deceleration, from the ion-exchange curve (Figure 8) for the K^+ substitution into Na−AlGe−GIS indicates 100% exchange might occur within 37.5 h.

Na^+ into K−AlGe−GIS only went to 10% (±2.5%) completion based on Rietveld refinement. The Na^+ for K−AlGe−GIS rate of ion exchange was much slower, and with use of a constant rate of deceleration, full exchange may have occurred after 1247 h. These results imply a preference of K^+ over Na^+ in the AlGe−GIS structure.

Since the AlGe−GIS structures contain a significant number of interstitial water molecules in addition to cations, the interaction between water and extraframework species may control the kinetics of ion exchange, especially when all the species of interest can geometrically fit in the pores of the molecular sieve. The subtle change in channel geometry between the *I*2/*a* and *C*2/*c* structures is not expected to affect the ion-exchange

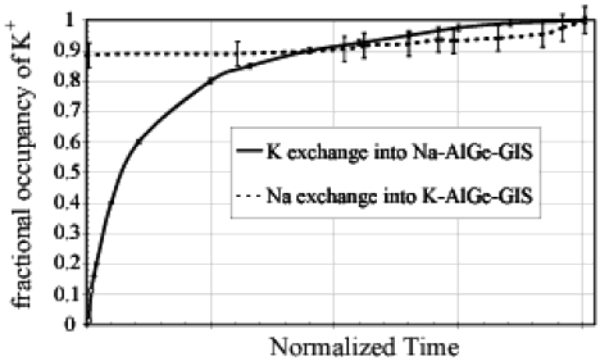

Figure 8. Refined site occupancy sums of all K^+ (K1−K6) for the K^+ into Na−AlGe−GIS ion exchange (solid line) and Na^+ for K−AlGe−GIS ion exchange (dashed line). Occupancies for Na^+ are not shown. Open circle data points represent occupancy sum of K^+ (K2, K4, K6) along the [$\bar{1}$01] channel. Time is normalized to account for the different experiment time durations and different solution drop rates.

processes because both cations (Na^+ and K^+) have been shown previously to easily fit in the pores of both end-member structures.[23] The ion exchange of K^+ and Na^+ in AlGe−GIS is not 100% reversible and this is interpreted to be due to the variation in water content between the two structures and the number of bonds each interstitial cation has with water. There are eight more water molecules in the Na−AlGe−GIS structure than in K−AlGe−GIS when compared in the *C*2/*c* basis. Since there are no unbound water molecules in the Na−AlGe−GIS framework, Na^+ bonds to more water than does K^+ in the superhydrated Na−AlGe−GIS (Table 2).

The higher coordination of Na^+ to water can be explained by the valence matching principle,[43−45] which states that the most stable structures will form when the Lewis acid strength of the cation closely matches the Lewis base strength of the anion. The Lewis acidity of K^+ and Na^+ are 0.13 v.u. and 0.16 v.u.[45] respectively, and H_2O has a Lewis base value of approximately 0.2 v.u.[43] Since the Lewis acidity of Na^+ more closely matches the Lewis base of H_2O, Na^+ has a stronger affinity to H_2O.

The relative strengths of Na^+/K^+ bonds to H_2O/framework O^{2-} can be approximated by using bond valence calculations[45] (Table 2), which estimates the amount of unit valence charge of the central ion that is contributed in bonding to its neighboring species. These calculations show that an interstitial cation with a higher coordination to H_2O than its ion-exchanged counterpart will have relatively weaker bonding interactions to the framework and thus be more easily exchanged.

In the structure solved by Tripathi et al.,[23] bond valence calculations for K^+ in K−AlGe−GIS (Table 2) show that the average total bond valence is 0.825 v.u. This assumes only first-coordination sphere bonding and that the bond valence pseudopotential is constant (b = 0.37 Å) as suggested by Brown and Altermatt.[46] The

(43) Hawthorne, F. C. *Acta Crystallogr. Sect. B−Struct. Commun.* **1994**, *50*, 481−510.
(44) Hawthorne, F. C. *Z. Kristallogr.* **1992**, *201*, 183−206.
(45) Brown, I. D. In *Structure and bonding in crystals*; O'Keeffe, M., Navrotsky, A., Eds.; Academic Press: New York, 1981; Vol. 2, pp 1−30.
(46) Brown, I. D.; Altermatt, D. *Acta Crystallogr. Sect. B−Struct. Commun.* **1985**, *41*, 244−247.

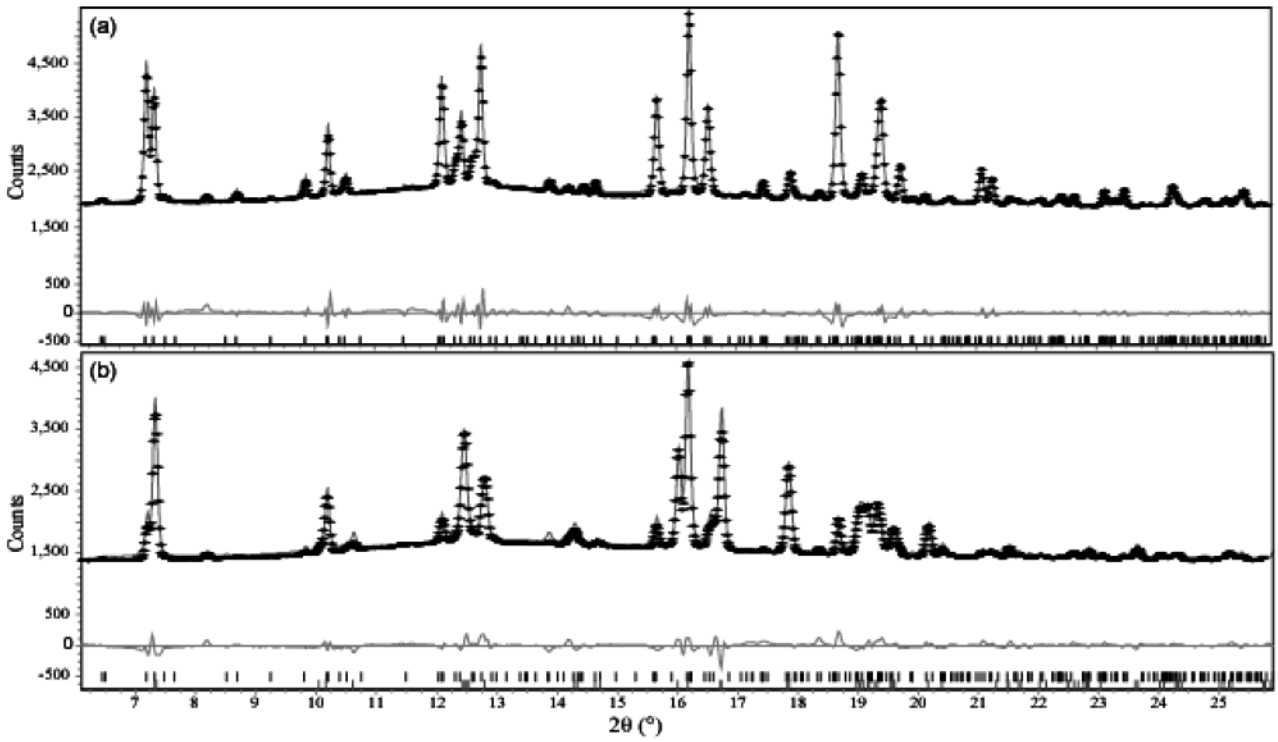

Figure 9. Rietveld refinement plots show the calculated (solid curve), experimental (dotted curve), and difference (solid curve on the bottom) for X-ray diffraction patterns of K^+ exchange into Na−AlGe−GIS at (a) time = 0 and (b) at time = 575 min.

Table 2. Bond Valence List for Na^+ and K^+ in Na−AlGe−GIS and K−AlGe−GIS, Respectively, to Framework O^{2-} and Interstitial H_2O

Na1	(v.u.)	Na2	(v.u.)	Na3	(v.u.)
O10	0.057	O1	0.168	O10	0.198
O35	0.101	(H_2O)O31	0.232	O8	0.15
O12	0.146	(H_2O)O34	0.218	(H_2O)O36	0.21
O4	0.156	(H_2O)O35	0.174	(H_2O)O30	0.205
(H_2O)O32	0.158	(H_2O)O32	0.073	(H_2O)O31	0.132
(H_2O)O34	0.166			(H_2O)O36	0.114
(H_2O)O33	0.241			(H_2O)O32	0.051
(H_2O)O33	0.39				

K1	(v.u.)	K2	(v.u.)
O3	0.138	O1	0.168
O4	0.132	O2	0.129
O1	0.108	O4	0.097
O2	0.064	O3	0.46
(H_2O)O21	0.194	(H_2O)O22	0.191
(H_2O)O21	0.147	(H_2O)O22	0.119
(H_2O)O22	0.042	(H_2O)O21	0.037

average bond valence of K^+ to water and O^{2-} are 0.365 v.u. and 0.423 v.u., respectively, suggesting K^+ has a stronger electronic interaction with framework anions than to interstitial water molecules. In contrast, the average total bond valence of Na^+ in Na−AlGe−GIS (Table 2) is 0.996 v. u., and the average bond valence to water and O^{2-} are 0.705 v.u. and 0.253 v.u., respectively. Bond valence calculations indicate that Na^+ has a weaker valence interaction with the framework than does K^+. Although the total average bond valence of Na^+ is higher than that for K^+, the ion exchange between Na^+ and K^+ will proceed in favor of K^+ because the K^+ to framework O^{2-} directly balances the negative charge on the framework. This agrees with the results of the experimental ion-exchange curve obtained (Figure 8). Similar methods using bond valence calculations to describe how readily cations ion exchange were performed by Park et al.,[47] who showed that the higher the total average bond valence around an interstitial cation, the less likely it would be to exchange. Bond valence calculations can provide a valuable guide to identify the weakest links for an interstitial species.

Although the exact transformation process between the *I*2/*a* and the *C*2/*c* unit cell remains uncertain, in situ time-resolved diffraction and bond valence studies suggest possible scenarios toward this transition. Our hypothesis is that Na^+ has a high-coordination hydration sphere in solution prior to entering the K−AlGe−GIS structure. This lowers the total bond valence that $Na-H_2O$ could directly contribute to neutralize the negative framework charge and does not favor its ion exchange into the AlGe−GIS framework. Also, the hydrated Na^+ would be stereochemically less likely to enter the channels due to the larger radius of its associated hydration sphere. The onset of the *C*2/*c* unit cell may have been a result of the experimental procedure since the flow-through cell is constantly refreshing the exchange solution with Na^+ and the K^+ that leaves the zeolite during ion exchange is not retained in the ion-exchange environment. This promotes the exchange for Na^+ and drives the substitution further.

Conclusion

Cation substitution of K^+ and Na^+ into the Na−AlGe−GIS and K−AlGe−GIS structures has been examined by time-resolved in situ XRPD. Site-selective ion exchange of K^+ into Na−AlGe−GIS along the [$\bar{1}$01] channel proceeded to 10% (±2%) K^+ exchange. Afterward, K−AlGe−GIS began to grow and subsequent structure refinements were consistent with a site-

(47) Park, S. H.; Kleinsorge, M.; Grey, C. P.; Parise, J. B. *J. Solid State Chem.* **2002**, *167*, 310−323.

independent ion exchange. The total K^+ substitution was modeled to 90% (±1%) completion based on Rietveld refinement of site occupancies. On the reverse exchange of Na^+ into K−AlGe−GIS, the *C*2/*c* unit cell formed at 4.5% (±3.5%) Na^+ substitution and total Na^+ exchange was refined to 10% (±2.5%). The preference of the AlGe−GIS framework for K^+ is interpreted to reflect the greater amount of bond valence that K^+ contributes to framework O^{2-}.

Time-resolved powder diffraction experiments require that data collection to be as short as possible while maintaining good quality data. In the case of materials as complex as those studied in this work however, lower angular and peak resolution, larger peak-to-background ratios, and poor counting statistics limit the information content. The use of judicious constraints and precise structure models for end-member compositions can partially compensate for the lack of high-resolution data. While we were able to refine extraframework cation occupancies at various stages of the ion exchange, we believe this study represents the current limits of in situ ion exchange with complex crystal structures such as microporous materials at second-generation synchrotron sources.

Acknowledgment. This work was supported by NSF Grant No. DMR-0095633 awarded to J.B.P. Research was carried out in part at the National Synchrotron Light Source, Brookhaven National Laboratory, which is supported by the U.S. Department of Energy, Division of Materials Sciences and Division of Chemical Sciences, under Contract No. DE-AC02-98CH10886. Thanks to Jennifer M. Cole and Ivor Bull for all their help.

CM034746I